Fast metastable hydrogen atoms from H₂ molecules: twin atoms

A. Trimèche[1], D. Houdoux[1], G. Rahmat[1], O. Dulieu[1], I.F. Schneider[1,2], A. Medina[4], G. Jalbert[3], F. Zappa[5], C.R. de Carvalho[3], R.F. Nascimento[6], N.V. de Castro Faria[3] and J. Robert[1]

[1]Laboratoire Aimé Cotton CNRS, Univ. Paris Sud 11, ENS Cachan, 91405 Orsay Cedex, France
[2]LOMC-FRE 3102-CNRS, Univ. du Havre, 25 rue Philippe Lebon, BP 540, 76058 Le Havre, France
[3]Instituto de Física, UFRJ, Cx. Postal 68528, Rio de Janeiro, RJ 21941-972, Brazil
[4]Instituto de Física, Universidade Federal da Bahia, Salvador, BA 40210-340, Brazil
[5]Departamento de Física, UFJF, Minas Gerais 36036-330, Brazil
[6]C.F.E. T. Celso Suckow da Fonseca, 25620-003, Petrópolis, RJ, Brazil

Abstract. It is a difficult task to obtain "twin atoms", *i.e.* pairs of massive particles such that one can perform experiments in the same fashion that is routinely done with "twin photons". One possible route to obtain such pairs is by dissociating homonuclear diatomic molecules. We address this possibility by investigating the production of metastable H(2s) atoms coming from the dissociation of cold H₂ molecules produced in a Campargue nozzle beam crossing an electron beam from a high intensity pulsed electron gun. Dissociation by electron impact was chosen to avoid limitations of target molecular excited states due to selection rules. Detectors placed several centimeters away from the collision center, and aligned with respect to possible common molecular dissociation channel, analyze the neutral fragments as a function of their time-of-flight (TOF) through Lyman-α detection. Evidence for the first time observed coincidence of pairs of H(2s) atoms obtained this way is presented.

1. Introduction

Two experimental devices dedicated to the study of the dissociation of an excited hydrogen molecule into twin hydrogen atoms in the 2s state have been developed at the *Laboratoire Aimé Cotton*, CNRS and at *Instituto de Fisica, U.F.R.J.*. The project aims at analyzing the conditions to maintain the spin coherence between two atomic fragments resulting from the same molecular state, namely an EPR pair [1], exploring the border between molecular physics and quantum information.

David Bohm proposed [2] that a pair of atoms, corresponding to a pair of spin-$\frac{1}{2}$ particles, coming from a molecular fragmentation could be used to implement the famous *gedankenexperiment* of Einstein, Podolsky and Rosen (EPR) [1]. His proposal intended to substitute the noncommuting observables x and p discussed in the EPR paper by the spin observables σ_x and σ_y, experimentally easier to deal with.

Nevertheless, despite the apparent simplicity of his proposal, actual EPR pairs were never done that way. Indeed, the first experiment by Wu and Shaknov in 1950 was on disintegration of positronium [3]. Later, Clauser and Shimony [4], Aspect, Dalibard and Roger [5] and Aspect, Grangier and Roger [6], among others, also used pairs of photons. If coincidence experiments are now common in atomic or molecular physics, the adjunction of the spin analysis of both fragments is not an easy task, and has not yet been successfully done [7].

The equivalent of such twin-photon experiments with atoms is of great interest because it poses several challenges to its theoretical description. A departing pair of atoms will browse the complex field of the molecular interactions from the short-distance (electrostatics and exchange) to the long-distance (Casimir-Polder interaction between moving atoms). The coherence of spin will therefore contain information related to these different interactions and its description should use dynamical terms related to the motion of the atoms. In Quantum Electrodynamics, the electromagnetic field is represented by functions belonging to the ordinary 3-dimensional physical space. In molecular physics a two body system is described in the 6-Dimensional configuration space, that have to be projected on the 3-D physical space. Most treatments focus mainly on the spin correlation tensor in order to bypass this problem [8]. The molecular description of atomic collisions gives a clue to go into this point and to compute the associated phase shifts [9]. In short, such an experiment could be used to observe and manipulate the phase of a dissociative molecular state, which is naturally an entangled one, and reveals in a non-trivial way all the dynamical complexity of the system.

Following U. Fano's method [8], one can formulate the natural entanglement in a dissociative molecular system along the following lines. For an isotropic dissociation, in S-wave, the asymptotic initial state is represented with the wave function $|\Psi\rangle$ involving the phase shift δ induced by the molecular interaction:

$$\langle \mathbf{R}_{CM}, r | \Psi \rangle \approx e^{i\mathbf{K}_c.\mathbf{R}_{CM}} \frac{sin(k_r\, r + \delta)}{k_r\, r} \,. \tag{1}$$

Where $\mathbf{R}_{CM}$ and $\mathbf{K}_c$ are the Center of Mass coordinate and momentum, r and k_r he relative coordinate and momentum. This can be re-written using the $\mathbf{r}_1$, $\mathbf{r}_2$ "laboratory" representation.

$$\langle \mathbf{r}_1, \mathbf{r}_2 | \Psi \rangle \approx e^{i\mathbf{K}_c.\frac{m_1 \mathbf{r}_1 + m_2 \mathbf{r}_2}{m_1 + m_2}} \frac{sin(k_r\,|\mathbf{r}_2 - \mathbf{r}_1| + \delta)}{k_r\,|\mathbf{r}_2 - \mathbf{r}_1|} \tag{2}$$

and without normalization

$$|\Psi\rangle \approx \frac{1}{2i}\left[e^{i\delta}|\mathbf{k}_1^-\rangle|\mathbf{k}_2^-\rangle - e^{-i\delta}|\mathbf{k}_1^+\rangle|\mathbf{k}_2^+\rangle \right] \tag{3}$$

where the ingoing $|\mathbf{k}_i^-\rangle$ and outgoing $|\mathbf{k}_i^+\rangle$ momenta for each particle $i = 1, 2$ of mass m_i are expressed as functions of the momenta of the center of mass $\mathbf{K}_c$ and of the relative vector $\mathbf{k}_r$:

$$|\mathbf{k}_1^{\pm}\rangle = |\frac{m_1\mathbf{K}_c \pm (m_1 + m_2)\mathbf{k}_r}{m_1 + m_2}\rangle, \tag{4}$$

$$|\mathbf{k}_2^{\pm}\rangle = |\frac{m_2\mathbf{K}_c \mp (m_1 + m_2)\mathbf{k}_r}{m_1 + m_2}\rangle \,. \tag{5}$$

A more general initial state, where flux normalization can be inclueed $|\varphi\rangle$ is described with respect to the center-of-mass and relative momenta such that:

$$|\varphi\rangle = \int C(\mathbf{K}_c', \mathbf{k}_r') \times |\Psi(\mathbf{K}_c, \mathbf{k}_r, \delta)\rangle d\mathbf{K}_c' d\mathbf{k}_r'. \tag{6}$$

The action of the two detectors A and B is modeled through the projection operators $\hat{D}_A$ and $\hat{D}_B$:

$$\hat{D}_A = \left[|\mathbf{k}_A\rangle_{11}\langle\mathbf{k}_A| \cdot \mathbf{1}_2 + \mathbf{1}_1.|\mathbf{k}_A\rangle_{22}\langle\mathbf{k}_A| \right] \tag{7}$$

$$\hat{D}_B = \left[|\mathbf{k}_B\rangle_{11}\langle\mathbf{k}_B| \cdot \mathbf{1}_2 + \mathbf{1}_1 \cdot |\mathbf{k}_B\rangle_{22}\langle\mathbf{k}_B| \right], \tag{8}$$

where $|\mathbf{k}_A\rangle_i$ and $|\mathbf{k}_B\rangle_i$ are the momentum states of particle i when hitting detector A and B, respectively, and $\mathbf{1}_i$ are the identity operator for particle i. The coincidence signal is expressed by the expectation value $\langle\hat{D}_A\hat{D}_B\rangle_{|\varphi\rangle}$ over the initial state $|\varphi\rangle$. In the general case $\mathbf{k}_A \neq \mathbf{k}_B$ as the two detectors can be aligned with respect to different directions with respect to the dissociation center. The calculation involves the vector $\mathbf{K}_{AB} = \frac{m_1\mathbf{k}_A - m_2\mathbf{k}_B}{m_1 + m_2}$ corresponding to particle 1 reaching detector A and particle 2 reaching detector B.

In the case of a homonuclear molecule ($m_1 = m_2$) we have $\mathbf{K}_{AB} = -\mathbf{K}_{BA}$ and the two detectors coincidence signal is thus expressed as:

$$\langle\hat{D}_A\hat{D}_B\rangle_{|\varphi\rangle} = \frac{1}{2}\cos(\delta' - \delta'')\Big\{\varrho(\mathbf{k}_A + \mathbf{k}_B, \mathbf{k}_A + \mathbf{k}_B; \mathbf{K}_{AB}, \mathbf{K}_{AB}) + \varrho(\mathbf{k}_A + \mathbf{k}_B, \mathbf{k}_A + \mathbf{k}_B; -\mathbf{K}_{AB}, -\mathbf{K}_{AB}))\Big\}$$
$$- \frac{1}{2}\cos(\delta' + \delta'')\Big\{\varrho(\mathbf{k}_A + \mathbf{k}_B, \mathbf{k}_A + \mathbf{k}_B; \mathbf{K}_{AB}, -\mathbf{K}_{AB}) + \varrho(\mathbf{k}_A + \mathbf{k}_B, \mathbf{k}_A + \mathbf{k}_B; -\mathbf{K}_{AB}, \mathbf{K}_{AB})\Big\}$$
$$\tag{9}$$

where $\varrho(k, k'; K, K')$ stands for $C(k, k'; K, K')$.

The meaning of the terms of the right-hand side of Eq. (9) is straighforward. Note first that the four terms imply center-of-mass momentum conservation through the $\mathbf{k}_A + \mathbf{k}_B$ term. The first two terms correspond to the diagonal part of the density matrix representative of the initial state, with the two sign possibilities for the inter-particle vector. The third and fourth term correspond to terms non-diagonal with respect to the relative momentum.

One can also recover the corresponding signal on each individual detector:

$$\langle\hat{D}_A\rangle_{|\varphi\rangle} = \int \langle\hat{D}_A\hat{D}_B\rangle_{|\varphi\rangle}d\mathbf{k}_B$$
$$\langle\hat{D}_B\rangle_{|\varphi\rangle} = \int \langle\hat{D}_A\hat{D}_B\rangle_{|\varphi\rangle}d\mathbf{k}_A. \tag{10}$$

Since the metastable 2s state of atomic hydrogen has a very long (122 ms) natural lifetime, the possibility of a fragmentation channel of H_2 into a pair of such metastable atoms would be perfectly suited for experiments, where manipulation of phase factors and the use of Stern-Gerlach interferometric techniques [10] is pursued, including time selection of events [11], delayed choice experiments [12] or double atom interferometry related to the quantum Zeno effect [13]. On the other hand, H_2 is the simplest neutral molecule, since it is made up of only four bodies. The complexity of symmetries by permutation and the spin multiplicity can be investigated by a convenient choice of isotopes.

The "super-excited" H_2^{**} states of interest, which belong to the so-called Q_2 branch, are embedded in the dissociation continuum of H_2^+ [14], and also interact with the ionic-covalent configurations $H^+ - H^-$. All these states are coupled and therefore the resulting complex phase shifts involved in the correlation tensor contain the pair properties shared by the twin atoms.

The structure of H_2 and the dynamics of its fragmentation channels are the subject of renewed studies both experimental, by synchrotron radiation or laser techniques or in ion beam experiment [15–17] via the study of dissociative recombination [18, 19], and theoretical, by *ab initio* calculations or by the molecular multichannel quantum defect theory [20–27]. They are also part of the dynamics of H(2s) Bose Einstein Condensates [28]. Despite the wealth of information on fragmentation of H_2, very little is known about critical quantities required to design a source of twin atoms from molecular hydrogen, since most of these studies are concerned with the production of ionic species. The impact energies as well as the impact parameters which would maximize the production of H(2s) pairs are not known and the corresponding cross sections have not been determined. The conditions to detect both
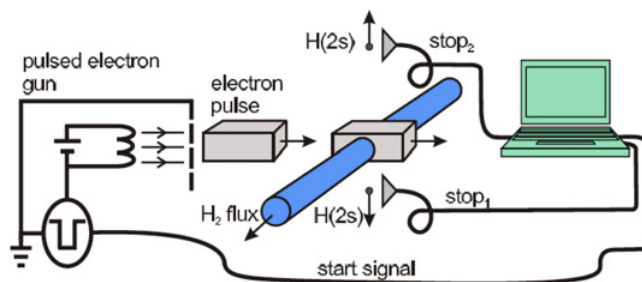
Figure 1. Schematic view of the experimental set-up (out of scale). Details are described in the text, as the detection system, with the two needles to produce the quenching and the Lyman-α filter.

atoms in coincidence, and at large macroscopic distances, involve a precise knowledge of the momentum transfer. As a first step on this path we present the measurements, with good time and space resolution, of fast H(2s) coming from the dissociation of cold H_2 induced by electrons with energies between 9.75 and 126 eV. In this energy range we swept the threshold for the production of fast H(2s) atoms. The obtained time-of-flight spectra allowed identifying the possible potential energy curves populated by electron impact. We also show, from the experimental coincidence results, the feasibility of our proposal of twin atoms production.

2. Experimental method

The basic lay-out of the experimental set-up (Fig. 1) is equivalent to the classical one [29] for time-of-flight (TOF) studies of H(2s) produced by electron impact on H_2, i.e., a hydrogen jet crossing at right angles with an electron beam. To reduce the spread of the velocity distribution of the hydrogen molecules, as well as to use well-defined initial molecular states and have sufficient target density, the hydrogen beam is produced by a Campargue-type supersonic jet source [30]. In the chamber where the collisions with the electrons take place, the pressure is maintained in the range 5×10^{-7} to 1.2×10^{-6} torr by a 2000 l/s diffusion pump. The measured mean velocity of the hydrogen molecules in the supersonic jet is 2.7 km/s and the jet temperature is about 3 K. Under these conditions, essentially all hydrogen molecules are in the molecular levels with vibrational quantum number $v = 0$ and rotational quantum number $J = 0$ and $J = 1$, with populations 1/3 and 2/3 respectively [31]. At the region where the molecular jet crosses with the electron beam, its diameter is approximately 3 mm and the flow is 10^{22} molecules per steradian per second, which corresponds to $(2.3 \pm 0.2) \times 10^3$ molecules per microsecond per cubic millimeter at the collision volume.

The pulsed electron gun consists of a $150 \, \mu m$ diameter thoriated-tungsten filament that together with a collimator, a grid and a Faraday cup produce and detect the electron beam that is approximately 2 mm × 6 mm wide and has a typical average current of 2 mA. The electron beam was pulsed by applying a negative voltage step, whose duration is on the range 0.2 to $1 \mu \sec$, to the filament that is otherwise maintained positive in order to reduce the electron background. The pulse rate was 10 kHz. The electron energy is given by the difference between the potential of the filament and the potential of the interaction region which has to be grounded in order to avoid the disappearance of H(2s) atoms through the coupling with radiatively decaying H(2p) states. The energy spread of the electron beam is estimated to be of about 6 eV, taking into account the voltage drop in the directly heated filament. This low resolution has no significant effect at high electron energies, as we do not intend to perform precise cross section measurements near the threshold.

The detection of the metastable H atoms is performed by a pair of specially devised detectors placed opposite to each other with respect to the plane defined by the electron and H_2 beams, at distances

which can be set from 6 to 25 centimeters away from the collision zone. This distance range precludes the arrival of excited H(2 p) atoms since, because of their lifetime of few nanoseconds, they should decay after traveling only a few millimeters, even in the case of the fastest fragments. Care was taken to place the detectors in positions consistent with the expected recoil of the superexcited H$_2^{**}$ molecules after collision with the electrons, as will be described later.

Each detector is composed of a channel electron multiplier of 10 mm aperture, oriented at right angles with respect to the atom trajectories in order to avoid counting photons originated by the de-excitation of short lived states. Emission of Lyman-α radiation (1216 Å) from the metastable atoms when they enter the detector is induced by quenching *via* 2s–2p mixing in an electrostatic field produced by two needles placed 4 mm in front of each multiplier cone. The Lyman-α radiation passes through a MgF$_2$ plate that shields the channeltron against other species such as electrons and ions. The entrance position of the metastable atoms is defined by a 2 mm diameter collimator placed at a distance of 2 cm upstream with respect to the needles.

Pulses from the detectors were separately pre-amplified and amplified by standard NIM electronics. After discrimination from electronic noise, the signals were fed as stop pulses of a "FAST ComTec" multi-stop time analyser card.

3. Experimental TOF spectra and collision kinematics

In Fig. 2 we present the experimental time-of-flight spectra obtained at electron collision energies between 9.75 and 126 eV. The detectors were placed 23 cm away from collision center as this position was a good compromise between counting rate and TOF resolution. The graphs represent the measurement of only one detector, irrespective of the detection on the other, normalized to the electron beam current and acquisition time. The vertical scales are changed in each case in order to make the features more apparent and comparable at all energies. The very high peak close to zero is due to the pick-up of the pulsing signal by the secondary-electron detectors, and is used for setting the correct "zero" for the flight times [43, 44].

The traditional classification of the metastable H(2s) atoms into "slow" (velocities of about 10 km/s) and "fast" (velocities of about 35 km/s) becomes evident, as well as their energetic thresholds: while the slow atoms coming from the simply excited states are visible in our entire energy range, the fast atoms, originating possibly from the Q$_1$ and Q$_2$ doubly-excited states, require electron energies higher than 30 eV.

In the literature there is quite no precise experimental information about the dissociation dynamics of superexcited H$_2^{**}$ energy levels that should dissociate in pairs of fast H(2s) fragments. In order to interpret our TOF spectra in more detail, one could try to transform the peak positions from time to kinetic energy of the molecular fragments, and this in turn to the Kinetic Energy Release (KER) in the molecular center-of-mass reference frame, from which one could identify the corresponding excited molecular states populated by the electron collision. If $\mathbf{V}_{\mathrm{Recoil}}$ is the final velocity of the H$_2$ molecule after electron impact in the laboratory reference frame, $\mathbf{V}_H$ is the velocity of the fragment in the center-of-mass frame of the molecule, and $\mathbf{R}_D$ is the distance vector between the collision zone and the detector, then

$$\mathbf{V}_{\mathrm{Recoil}} + \mathbf{V}_H = \frac{\mathbf{R}_D}{TOF} = \mathbf{V_D} \tag{11}$$

from which we get

$$KER = 2 \times \frac{1}{2} M_H \mathbf{V}_H^2 = M_H (\frac{\mathbf{R}_D}{TOF} - \mathbf{V}_{\mathrm{Recoil}})^2 \tag{12}$$

where $\mathbf{V_D}$ is the apparent velocity of the H atom in the laboratory reference frame. In order to determine $\mathbf{V}_H$, the amount of recoil of the H_2 molecules due to the impact of the electrons in the particular
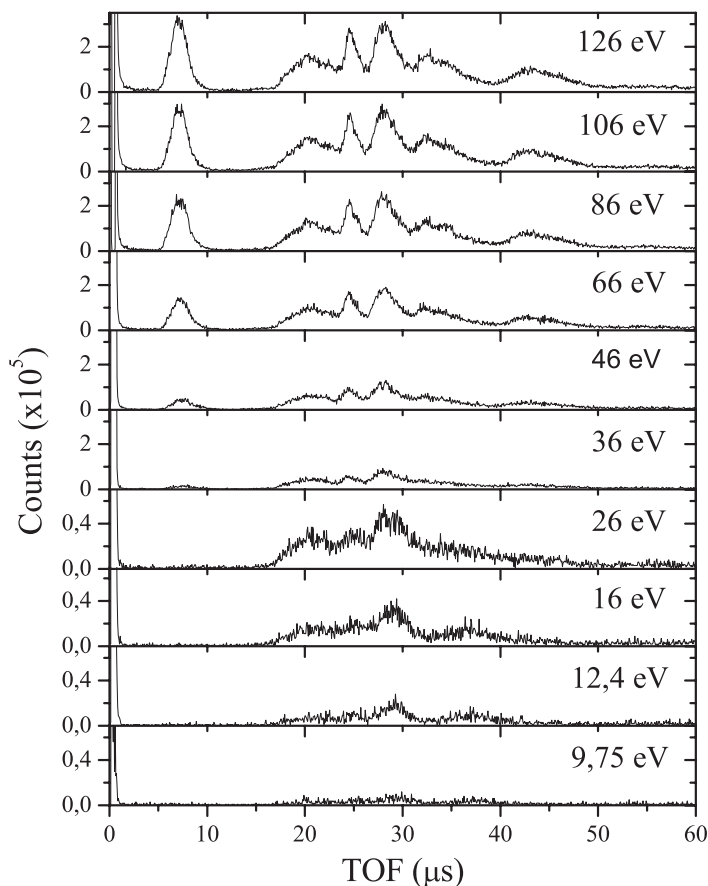
Figure 2. Time of flight spectra of H(2s) atoms dissociated from H_2^{**} molecules by electron impact with electron energies from 9.75 to 126 eV.

case of metastable H(2s) production has to be known. A completely inelastic knock-on collision of a 120 eV electron, for instance, could contribute to the molecule's final velocity as much as 2/3 of its initial velocity in the supersonic beam. In order to evaluate recoil possibilities one has to take care of the angular differential cross sections for electronic excitation by electron scattering, in the specific case of the states that contribute to our signal. Angular differential cross sections for H_2 excitation by electron impact are known for a variety of lower lying electronic states [32], but for metastable H(2s) pair production it is not known.

The graphic representation of the collision kinematics taking in account energy and momentum conservation, the "Newton Diagram", is presented in Fig. 3 in the case of 120 eV electron colliding at right angles with the H_2 supersonic beam. In the unrestricted case when any scattering angle is possible, the final recoil velocity vector of the target can sweep the whole surface of a sphere centered at the end of the CM velocity vector. The radius of the sphere is the magnitude of the electron momentum in the center of mass frame, after the collision, divided by the target mass. If the momentum vector is reduced due to inelasticity of the collision, the radius of the sphere gets proportionally smaller.

A reasonable assumption to the recoil velocity, in the absence of other information, is that it is approximately the same as the CM velocity. The uncertainty associated with this approximation can be evaluated graphically as is illustrated in Fig. 3b. For clarity the figure is out of scale. Thanks to the fact
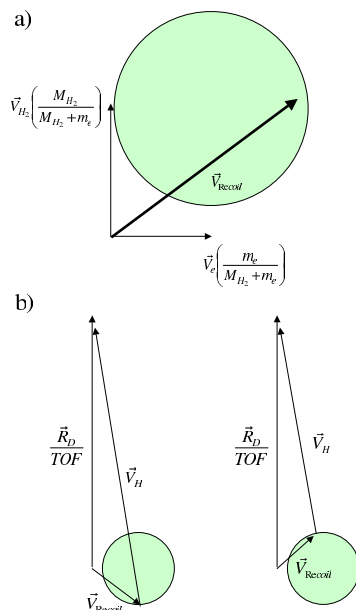
a)

b)

Figure 3. a) Diagram representing the possible recoil velocities for the H_2 molecule after impact of 120 eV electrons in the unrestricted case when the final velocity vector can sweep the whole volume of the circle whose radius depends on the inelasticity of the collision. (b) Diagram representing the possibilities for $\mathbf{V_H}$ consistent with detector position and measured Time of Flight of "fast atoms" for two extreme H_2 recoil vectors.

that the magnitude of $\mathbf{V_D}$, roughly 35000 m/s in the center of the "fast atoms" peak, is much larger than any possible $\mathbf{V_{Recoil}}$, the uncertainty in the KER determination is less than 8%. The width that can be attributed to this approximation, as obtained also by Monte Carlo simulation, is still 3 to 4 times smaller than the width of the TOF peak in the fast atom region. Therefore the TOF peak, in respect to both width and position, contains indeed information on the KER of the dissociation processes as will be discussed in more detail in the following section.

4. Fast H(2s) atoms

Molecular potential energy surfaces are not easily deduced from experimental data. The molecule complexity explains the existence of only very few direct measurements, even for small regions of the surface [33]. The theoretical situation is somewhat more comfortable than its experimental counterpart, as can be observed in literature. Nevertheless, Spezeski *et al*. [34] have achieved a complete study of the H_2 curves, even though the resolution of their spectra does not allow, for example, the separation of the slow H(2s) atoms. More recently Aoto *et al*. [35] show evidence, beyond the Q_1 and Q_2 states, for the observation of Q_3 and Q_4 doubly-excited states. By photodissociation, the excited energy levels allowed by the selection rules are the $^1\Sigma_u^+$ and the $^1\Pi_u$. Sanz-Vicario *et al*. [36] have developed a non-perturbative time-dependent method to describe autoionization of H_2 doubly-excited states and its manifestation in dissociative and non-dissociative ionization when the molecule interacts with femtosecond xuv laser pulses. They found that the states which photodissociate in H(2s) are the $1Q_1\,^1\Sigma_u^+$ and the $1Q_2\,^1\Pi_u$. On the other hand, Glass-Maujean *et al*. [37] modeled experimental cross section data in order to quantify the competition between the various decay channels and to try to get information on the dynamics of the different doubly excited states. To build up the H(2s) cross section, they used the contributions of the $2Q_1\,^1\Sigma_u^+$, $(1,4,5)\,Q_2\,^1\Pi_u$, $H_2^+(2s\sigma_g)$ and the $2Q_3\,^1\Pi_u$ and they observed that
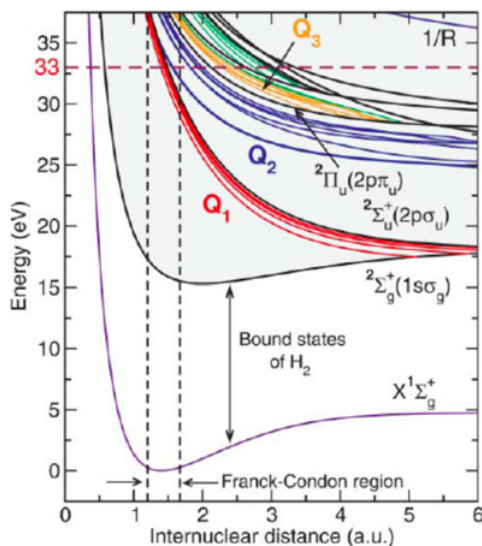
Figure 4. Potential energy curves as a function of inter-atomic distance for H_2 below and above ionization threshold. The relevant Q_1 and Q_2 family of states are represented. Figure extracted from reference [25].

the $(4, 5)$ Q_2 $^1\Pi_u$ gives a bigger contribution for the cross section. On the other hand, Jonsell *et al.* [38] were interested in the study of long-range interactions between two H(2s). According to them these atoms can originate from a molecular Q_2 doubly excited state of either $^1\Sigma_g^+$ or $^3\Sigma_u^+$ symmetry only, which is consistent with the rule determined by Wigner and Witner from group theory [39].

Extensive calculations of the doubly excited states Q_1 and Q_2 were done by I. Sánchez and F. Martín [23, 40, 41] in the framework of the Born-Oppenheimer approximation. The problem they were interested in was the representation of the electronic continuum for a fixed position of the nuclei. These doubly-excited states manifest themselves as resonances in the continuum spectrum of H_2 and the method to calculate resonance parameters was based on the Feshbach formalism [42]. We show in Figs. 5 and 6 the five lowest theoretical energy curves corresponding to their calculations for the Q_1 and Q_2 states, where the number represents the order in the symmetry.

As already explained, for the fast H(2s) atoms we have good kinematics resolution, so that the width and position of the fast atoms peak has to be associated with the various potential energy curves that dissociate into H(2s) + H(nl). If we could separate the different contributions, together with the wave function of the first vibrational level of H_2 [45], it would be possible to confirm or construct part of the related potential energy curves in the Franck-Condon region. For simplicity, however, instead of trying to solve this "inverse problem", in the present work we make use of the calculated doubly excited states Q_1 and Q_2 and the Method of Reflection [46] in order to match our experimental results by sampling different possibilities for the contribution of each state.

In Figs. 5 and 6, we present the KER peaks obtained for the different possible states by reflecting the ground state wave function of H_2 on the excited-state potential energy curves of reference [23]. On the right vertical axis these are compared to our experimental spectra after converting TOF coordinates into kinetic energy ones in the center of mass frame. However, the reflected peaks do not take into account the relative probabilities of the different channels. It means that their amplitudes do not correspond to their true contribution and we should analyze only the relative energy intervals.

We observe that in the majority of the Q_2 cases, there is a good agreement between the experimental value and those obtained from reflections, the opposite happening with the Q_1 cases. We can notice
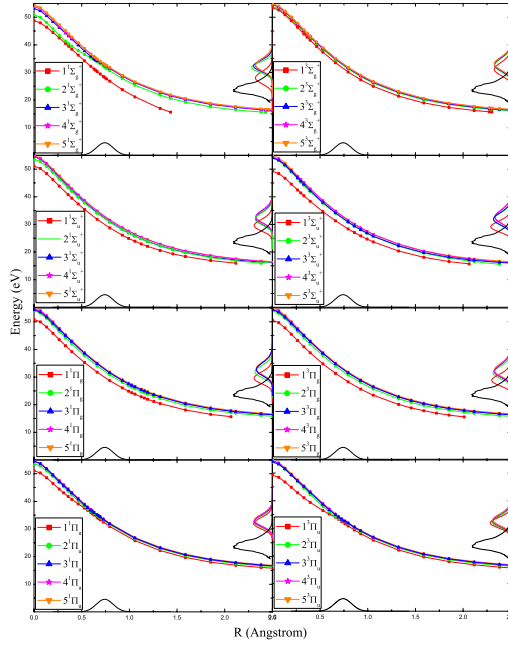
Figure 5. Results of the construction of the distribution of the possible H(2s) fast peak from H_2 by the reflection method. The continuous curve in the vertical axis is the experimental peak in center of mass kinetic energy coordinates. It is also shown the square of the wave function of the lowest vibrational level (lower state) and the Q_1 doubly excited states [23] (upper state).

in Fig. 5 that all Q_1 reflected peaks are in the larger energy range and are not centered inside the experimental peak, which means that if they had to contribute to the spectrum, it would be with a much smaller cross section. The reflection of the Q_2 states in Fig. 6 is not conclusive as most levels can apparently contribute to the whole energy range of the H(2s) fast peak.

5. Coincidence results

In our search for the observation of twin atom pairs [48], we have set up the detectors and acquisition electronics to perform data acquisition in the so-called "coincidence" mode in order to detect $\langle \hat{D}_A \hat{D}_B \rangle_{|\varphi\rangle}$. This means that the electronics only records the TOF of incoming particles if for a same starting pulse there are signals appearing on both detectors within the sweep time. Since the geometrical constraints are quite severe for this kind of event, to increase the detection solid angle, we have chosen to change the detectors configuration. In these experiments the collision center is in direct view of the channeltron cones, they are shielded by a double grid system, so that no stray electric field are present in the free flight zones. The upper detector at a distance of 67 mm and the lower detector 58 mm. The different distances are chosen to avoid that true counts would overlap the region where it could appear noise picked up simultaneously by both detectors. Care has to be taken to displace each detector, in the plane parallel to the plane defined by the electron and supersonic jet beams, so that their positions are consistent with the recoil kinematics of the H_2 molecules as was explained in Sect. 3: given a certain detector position in the upper plane consistent with $\mathbf{V}_{\text{Recoil}} + \mathbf{V}_H$, the other detector must be positioned at $\mathbf{V}_{\text{Recoil}} - \mathbf{V}_H$. This configuration where the detectors are at an average angle of $3°$ with respect to the perpendicular to the collision plane revealed to be the most favorable to detect any signal. This position was found experimentally at Rio, and confirmed in the Orsay experiment. It corresponds to fragment
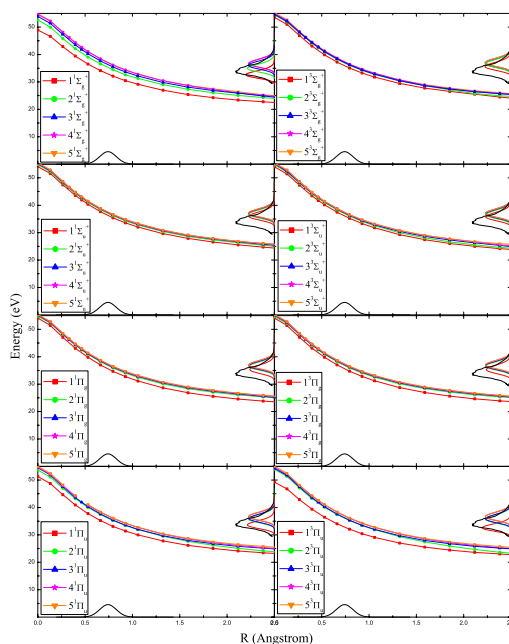
Figure 6. Results of the construction of the distribution of the possible H(2s) fast peak from H_2 by the reflection method. The continuous curve in the vertical axis is the experimental peak in center of mass kinetic energy coordinates. It is also shown the square of the wave function of the lowest vibrational level (lower state) and the Q_2 doubly excited states [23] (upper state).
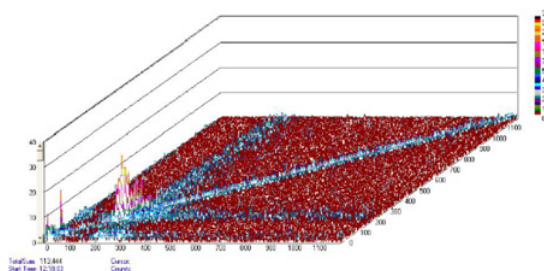

Figure 7. First successful coincidence obtained in Rio with 100 eV electron on a hydrogen cell. The detectors protected with a MgF_2 window were placed at 20 mm from the interaction center. The fist contribution in the diagonal arise from the (2 p,2 p) mechanism, the second from the (2s–2s) mechanism.

ejection somewhat faster than was expected with a simplified reasoning from the existing theoretical curves.

In Fig. 7 we present the raw results of the first successful coincidence experiment using 100 eV electrons. The vertical scale of the graph is the TOF channel recorded by the detector closer to the collision volume and the horizontal scale is the TOF channel recorded by the detector further away. The number of counts is depicted by the gray scale used to paint the coincidence points: the darker the point the higher the number of counts in a relative scale. One can see that there are events scattered pretty much throughout the entire coincidence space, with some islands with higher number of counts.
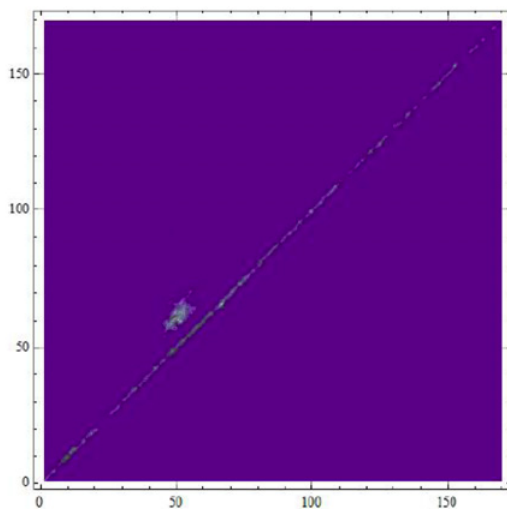
Figure 8. 2D map coincidence spectrum for an electron energy of 80 eV, diagonal line: electronic noise, upper part: signal corresponding to pair of metastable H atoms.
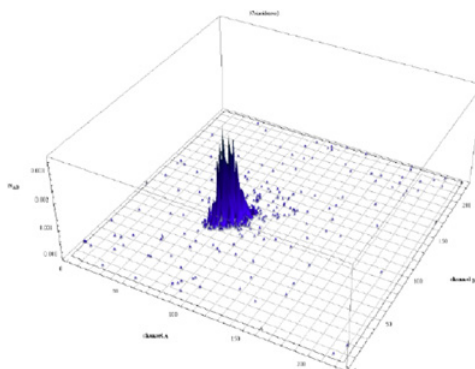

Figure 9. 2D map coincidence spectrum for an electron energy of 200 eV, upper part: signal corresponding to pair of metastable H atoms.

Results obtained in Orsay with the cold beam of molecular hydrogen are shown in Fig. 8 for an electron incident energy of 80 eV. The coincidence peak clearly appears in the upper part of the 2D map the central line corresponding to electronic noise.

Results for 200 eV electron energy are shown in Fig. 9. The detected coincidence peak remains and its position is very close to that of the 80 eV experiment. It was not possible to maintain the experimental parameters stable during a sufficient period to get the cross section of the process with respect to the electron energy.

In order to evaluate the background induced by random coincidences [47], we have performed an experiment where we have registered the signal maps corresponding to two successive electron gun impulses. In that case one can expect true coincidences only for the acquisition period corresponding to the same electron gun impulse. This result is clearly seen in 10.

Next we have projected the coincidence spectra on the non-coincidence ones in order to identify the TOF range were this process occurs, see Fig. 11. The twin metastable H atoms appear on the high energy
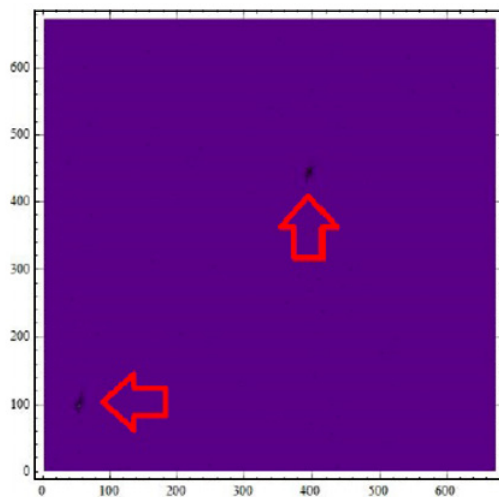
Figure 10. $4 \times 2D$ maps, electron energy 150 V. Anti diagonal 2D maps: arrows, coincidence spectra arising only when the detection times correspond to the same quantum event (i, i) and (i + 1, i + 1). Diagonal 2D maps: the detection times correspond to different quantum events (i, i + 1) and (i + 1, i). This map gives a qualitative information on the random coincidence noise which is very low.
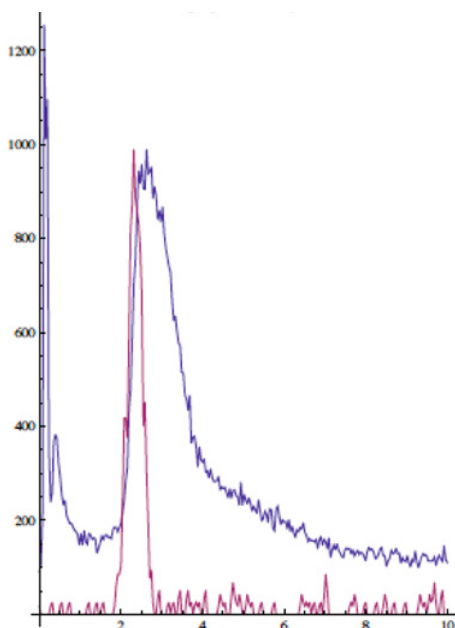

Figure 11. TOF spectra. Blue line: signal obtained in one detector. Red line: projection from the coincidence 2D map.

part. A precise determination of the energy where this process occurs and the associated inversion of the projection method are difficult to perform because the actual flight path of the atoms from the dissociation center to the detection zone is somewhat imprecise. Nevertheless rough analysis allows one to infer an energy range between 10 eV to 12 eV.

6. Conclusions

The aim of this paper is to study the production of pairs of fast H(2s) atoms coming from the fragmentation of the H_2 molecule by electron impact. As a first step, we have measured the H(2s) time-of-flight spectra for various incident electron energies, which allowed us to gain better understanding of the behavior of the differential cross sections involved. In a second step we investigated using the available theoretical potential energy curves the doubly-excited states of the molecule which can dissociate in at least one fast H(2s) atom. For this, the method of reflection has been shown to be very valuable, especially since the kinematics is determined in our experiment essentially by the potential energy curves of the relevant molecular states. Finally, we present for the first time evidence of the detection of twin H(2s) atoms in coincidence. The assignment of the molecular states associated to this phenomena is still in progress as precise determination of dissociation energies is needed. This implies an improved determination of the path length from the dissociation center to the actual detection zone. Up to now this process occurs at higher dissociation energies than those corresponding to the average energy of the "fast" peak. Other improvements towards spin sensitive detection of the products involve the optimisation of the rate of atoms associated to this twin atoms process.

References

[1]   A. Einstein, B. Podolsky, and N. Rosen, Phys. Rev. **47**, 777 (1935)

[2]   D. Bohm, *Quantum theory*, Eglewood Cliffs, NJ: Prentice-Hall (1951)

[3]   C. S. Wu, and I. Shaknov, Phys. Rev. **77**, 136 (1950)

[4]   J. F. Clauser, and A. Shimony, Rep. Prog. Phys. **41**, 1881 (1978)

[5]   A. Aspect, J. Dalibard, and G. Roger, Phys. Rev. Lett. **49**, 1804 (1982)

[6]   A. Aspect, P. Grangier, and G. Roger, Phys. Rev. Lett. **49**, 91 (1982)

[7]   E.S. Fry and T. Walther, Adv.Atom.Mol.Opt.Phys. **42** (2000); J. Koperski and E.S. Fry, J. Phys. B: At. Mol. Opt. Phys. **39**, S1125 (2006)

[8]   U. Fano, Rev. Mod. Phys. **55**, 855 (1983); M.O. Scully, N. Erez and E. S. Fry, Phys. Lett. A **347**, 56 (2005)

[9]   U. Fano, Rep. Prog. Phys. **46**, 97 (1983)

[10] J. Robert, Ch. Miniatura, O. Gorceix, S. Le Boiteux, V. Lorent, J. Reinhardt and J. Baudon, J. Phys. II (France) **2**, 601 (1992); Ch. Miniatura, J. Robert, O. Gorceix, V. Lorent, S. Le Boiteux, J. Reinhardt, and J. Baudon, Phys. Rev. Lett. **69**, 261 (1992); S. Nic Chormaic, V. Wiedemann, Ch. Miniatura, J. Robert, S. Le Boiteux, V. Lorent, 0. Gorceix, S. Feron, J. Reinhardt, and J. Baudon, J. Phys. B **26**, 1271 (1993); M. Boustimi, V. Bocvarski, B. Viaris de Lesegno, K. Brodsky, F. Perales, J. Baudon, and J. Robert, Phys. Rev. A **61**, 033602 (2000)

[11] B. J. Lawson-Daku, R. Asimov, S. N. Chormaic, O. Gorceix, Ch. Miniatura, J. Robert, and J. Baudon, Phys. Rev. A **52**, 2457 (1995)

[12] B. J. Lawson-Daku, R. Asimov, O. Gorceix, Ch. Miniatura, J. Robert, and J. Baudon, Phys. Rev. A **54**, 5042 (1996)

[13] R. Mathevet, K. Brodsky, J. Baudon, R. Brouri, M. Boustimi, B. Viaris de Lesegno, and J. Robert, Phys. Rev. A **58**, 4039 (1998)

[14] A. Lafosse, M. Lebech, J. C. Brenot, P.M. Guyon, L. Spielberger, O. Jagutzki, J. C. Houver, and D. Dowek, J. Phys. B: At. Mol. Opt. Phys. **36**, 4683 (2003)

[15] A. Al-Khalili et al., *J. Chem. Phys.* **121**, 5700 (2004)

[16] D. Zajfman, A. Wolf, D. Schwalm, D. A. Orlov, M. Grieser, R. von Hahn, C. P. Welsch, J. R. Crespo Lopez-Urrutia, C. D. Schröter, X. Urbain and J. Ullrich, J. Phys.: Conf. Ser. **4**, 296 (2005)

[17] V. Zhaunerchyk, A. Al-Khalili, R.D. Thomas, W.D. Geppert, V. Bednarska, A. Petrignani, A. Ehlerding, M. Hamberg, M. Larsson, S. Rosén, and W.J. van der Zande, *Phys. Rev. Lett.* **99**, 013201 (2007)

[18] W. v.d. Zande (editor), *J. Phys.:Conference. Series* **192** (2009)

[19] M. Larsson and A. E. Orel, "Dissociative Recombination of Molecular Ions", Cambridge University Press (2008)

[20] H.J. Wörner, S. Mollet, Ch. Jungen, and F. Merkt, Phys. Rev. A **75**, 062511 (2007)

[21] E. Melero García, J. Álvarez Ruiz, S. Menmuir, E. Rachlew, P. Erman, A. Kivimäki, M. Glass-Maujean, R. Richter, and M. Coreno, J. Phys B: At. Mol. Opt. Phys **39**, 205 (2006)

[22] J. D. Bozek, J. E. Furst, T. J. Gay, H. Gould, A. L. D. Kilcoyne, J. R. Machacek, F. Martín, K. W. McLaughlin, and J. L. Sanz-Vicario, J. Phys. B: At. Mol. Opt. Phys. **39**, 4871 (2006)

[23] I. Sánchez and F. Martín, J. Chem. Phys. **106**, 7720 (1997); J. Chem. Phys. **110**, 6702 (1999)

[24] Y. V. Vanne, A. Saenz, A. Dalgarno, R. C. Forrey, P. Froelich, and S. Jonsell, Phys. Rev. A **73**, 062706 (2006)

[25] F. Martín, J. Fernández, T. Havermeier, L. Foucar, Th. Weber, K. Kreidi, M. Schöffler, L. Schmidt, T. Jahnke, O. Jagutzki, A. Czasch, E. P. Benis, T. Osipov, A. L. Landers, A. Belkacem, M. H. Prior, H. Schmidt-Böcking, C. L. Cocke, R. Dörner, Science **315**, 629 (2007)

[26] A. Giusti-Suzor, *J. Phys. B: At. Mol. Phys.* **13**, 3867 (1980)

[27] O. Motapon, F. O. Waffeu Tamo, X. Urbain and I. F. Schneider, *Phys. Rev.* **A77**, 052711 (2008)

[28] D.G. Fried, T.C. Killian, L. Willmann, D. Landhuis, S.C. Moss, D. Kleppner, and T.J. Greytak, Phys. Rev. Lett. **81**, 3811 (1998); T.C. Killian, D.G. Fried, L. Willmann, D. Landhuis, S.C. Moss, T.J. Greytak, and D. Kleppner, Phys. Rev. Lett. **81**, 3807 (1998); D. Landhuis, L. Matos, S.C. Moss, J.K. Steinberger, K. Vant, L. Willmann, T.J. Greytak, and D. Kleppner, Phys. Rev. A **67**, 022718 (2003)

[29] M. Leventhal, R. T. Robiscoe, and K. R. Lea, Phys. Rev. **158**, 49 (1967)

[30] R. Campargue, J. Phys. Chem. **88**, 4466 (1984)

[31] A. Lebehot, J. C. Lemonnier and A. Marette, Rarefied Gas Dynamics, S.S Fischer, London, 1981

[32] M. J. Brunger, S. J. Buckman, Phys. Rep. **357** (2002) 215

[33] M. Barbatti, L. P. G. de Assis, Ginette Jalbert, L. F. S. Coelho, I. Borges Jr. and N. V. de Castro Faria, Phys. Rev. A **59**, 1988 (1999)

[34] J. J. Spezeski, O. F. Kalman, and L. C. McIntyre, Jr, Phys. Rev. A **22**, 1906 (1980)

[35] T. Aoto, Y. Hikosaba, R. I. Hall, K. Ito, J. Fernandez, and F. Martin, Chem. Phys. Letters **389**, 145 (2004)

[36] J. L. Sanz-Vicario, H. Bachau and F. Martín, Phys. Rev. A **73**, 033410 (2006)

[37] M. Glass-Maujean and H. Schmoranzer, J. Phys. B **38**, 1093 (2005)

[38] S. Jonsell, A. Saenz, P. Froelich, R. C. Forrey, R. Côté and A. Dalgarno, Phys. Rev. A **65**, 042501 (2002)

[39] E. Wigner and E. E. Witmer, Z. Physik **51**, 859 (1928)

[40] S. L. Guberman, *J. Chem. Phys.* **78**, 1404 (1983)

[41] J. Tennyson, *At. Dat. Nucl. Data Tables* **64**, 253 (1996)

[42] H. Feshbach, Ann. Phys. (N.Y.) **19**, 287 (1962)

[43] A. Medina, G. Rahmat, C. R. de Carvalho, G. Jalbert, F. Zappa, R. F. Nascimento, R. Cireasa, N. Vanhaecke, Ioan F. Schneider, N. V. de Castro Faria and J. Robert, J. Phys. B: At. Mol. Opt. Phys. **44**, 215203 (2011)

[44] A. Medina, G. Rahmat, G. Jalbert, R. Cireasa, F. Zappa, C. R. de Carvalho, N. V. de Castro Faria and J. Robert, Eur. Phys. J. D **66**, 134 (2012)

[45] W. Kolos and L. Wolniewicz, J. Chem. Phys. **43**, 2429 (1965)

[46] J. G Winans and E. C. G. Stueckelberg, Proc. Nat. Acad. Sci. **4**, 867 (1928); H. D. Hagstrum and J. T. Tate, Phys. Rev. **59**, 354 (1941)

[47] C. Eckart and F. R. Shonka, Phys. Rev. **53** (1938) 752

[48] J. Robert, F. Zappa, C. R. de Carvalho, Ginette Jalbert, R. F. Nascimento, A. Trimeche, O. Dulieu, Aline Medina, Carla Carvalho, and N. V. de Castro Faria, Phys. Rev. Lett. **111**, (2013) 183203